Light-Driven Unidirectional Liquid Motion on Anisotropic Gold Nanorod Arrays

*Mehmet Yilmaz, Hamit Bugra Kuloglu, Hakan Erdogan, Saime Sebnem Cetin, Mustafa Selman Yavuz, Gozde Ozaydin Ince, and Gokhan Demirel**

Microfluidic systems, which are related to manipulation of a small amount of liquid motion, have attracted increasing interest during the past decade.[1–4] In this respect, they have been widely used for various applications including biological analysis, chemical synthesis, and optics.[5–7] However, most of the microfluidic systems suffer from the complex fabrication methods and controlling the fluid motion in channels, which can be generated via electrokinetic, mechanical, hydraulic, or pneumatic forces and, therefore, usually require the use of external transducers such as pumps, valves, or electrodes.[8–10] To overcome such drawbacks, a number of paradigms based on an external stimulus to drive small amount of liquids either confined in a channel or an open environment have been proposed, including focused acoustic waves, light, electrical stimulation, and chemical or temperature based Leidenfrost ratchet.[1,11–13] Among them, light has opened up new avenues for the facile manipulation of liquid motion since it enables simple yet precise tunability, contactless stimulation, and excellent spatial resolution.

Fundamentally, transportation of a liquid through photoirradiation relies on the generation of a gradient in various interfacial phenomena, including surface free energy, wettability, crystal alignment, or dispersibility.[12,14–17] Thus, when chemical structures on a surface are altered photochemically, which leads to the generation of a surface free energy gradient, liquid motion can be controlled and guided. Such a surface free energy gradient can be generated by illuminating a substrate with photoresponsive wettable features. Basically, these kinds of substrates are classified into two groups. The first one is the inorganic substrates, such as titanium dioxide (TiO_2) and zinc oxide (ZnO), which show photoresponsive behaviors. Although the droplet motion on such surfaces has been recently demonstrated,[18–20] direct manipulation of liquid motion in a controlled manner by light on an inorganic substrate has not yet been reported. Unlike inorganic materials, organic molecules, such as azobenzenes, spiropyran molecules, or rotaxens, which exhibit a reversible molecular transformation between two states upon light illumination, have distinct advantages related to their chemical modification abilities and reaction diversities.[21–23] These light-induced molecular transformations cause various changes, including surface energy, absorption property, dielectric constant, and geometric molecular structure. In this context, such organic molecules have been widely utilized for the manipulation of surface wettability through light.[12,19,20] However, up to now, only the flow of a few organic liquids can be manipulated on surfaces decorated with photoresponsive organic molecules. Thus, to achieve the manipulation of either water or organic liquids in a controlled manner, novel materials and concepts are still desperately needed.

In the present study, we proposed a simple concept for the control of liquid motion through light illumination. The developed concept does not only allow the motion and guidance of water via light illumination, but also allows the flow rate and direction of the liquid to be easily controlled. The proposed system consists of two main components (**Figure 1**a). The first of these components is an array of 3-D gold nanorods (AuNRs) that possess directional characteristics. These structures with plasmonic properties generate thermal energy through photothermal phenomenon. Another significant aspect of the proposed concept is that it includes a temperature-sensitive polymeric layer (poly(*N*-isopropylacrylamide)-PNIPAAm) that conformally covers the surface of the AuNRs. This layer serves to adjust and manipulate the surface free energy of the substrate that converts light energy into thermal energy. This, in turn, creates a surface gradient that enables the control of the liquid motion. In this context, we first fabricated AuNR arrays as a photothermal substrate via oblique angle deposition (OAD) approach, where the deposition angle (α) of gold is 5°. Recently, we have reported that the AuNR arrays fabricated at $\alpha = 5°$ have low-density gold nanostructure array compared to 10° and 20° of deposition angles.[24] An increment at deposition angle causes an increase in structural density. As a result, the gaps between the nanostructures, which provide the air to be trapped beneath liquid droplets, are reduced and directional wetting abilities correspondingly decrease. Thus, in this work, we have fabricated gold nanostructures at $\alpha = 5°$. Figure 1b,c shows the scanning electron microscope (SEM) images of fabricated AuNRs. It is obvious that the Au films have ordered and tilted gold nanostructures. The density and tilt angle (β) of the fabricated Au nanostructures were calculated from SEM images by using freeware IMAGEJ software as 6.12×10^8 nanorod.cm^{-2} and 41° ± 4°, respectively. The

Dr. M. Yilmaz, H. Erdogan, Dr. S. S. Cetin, Prof. G. Demirel
Bio-inspired Materials Research Laboratory (BIMREL)
Department of Chemistry
Gazi University
06500 Ankara, Turkey
E-mail: nanobiotechnology@gmail.com
H. B. Kuloglu, Prof. G. O. Ince
Faculty of Engineering and Natural Sciences
Sabanci University
34956 Istanbul, Turkey
Prof. M. S. Yavuz
Department of Metallurgy and Materials Engineering
Selcuk University
42075 Konya, Turkey

DOI: 10.1002/admi.201500226

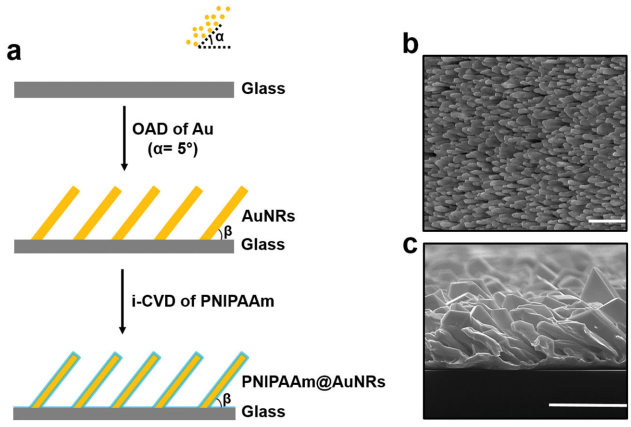

Figure 1. a) Schematic illustration of the fabrication process of PNIPAAm-coated AuNR arrays based on oblique angle deposition (OAD) and initiated-chemical vapor deposition (i-CVD) techniques (α and β indicates the deposition angle of gold and tilt angle of fabricated AuNRs, respectively), b) top-view and c) cross-section SEM images of a fabricated platform (scale bars = 1 μm).

average lengths of nanostructures were also found to be ≈800 nm. The diameters of these nanorods, however, showed a broad distribution, ranging from 70 to 300 nm. Furthermore, the structural properties including length, density, and tilt angle of the fabricated AuNRs could be easily manipulated by controlling the deposition parameters in order to tune their plasmonic behaviors.[24, 25]

Using a spectroscopic ellipsometry, we evaluated the plasmonic properties of fabricated AuNR arrays. **Figure 2** shows the variations of ellipsometric variables (Ψ and Δ) and pseudo-dielectric constants (real ($\langle\varepsilon_{real}\rangle$) and imaginary ($\langle\varepsilon_{Im}\rangle$) parts) for AuNR arrays before PNIPAAm coating with respect to the direction of incoming light at 65° of incident angle. To understand the homogeneity of fabricated films, ellipsometric analysis has also been carried out at varying angles of incidence (see Figure S1, Supporting Information). We found that fabricated AuNR arrays reveal an obvious optical anisotropy depending on direction of incoming light. In the case of anisotropic axis, the amplitude (Ψ) spectrum shows a sharp dip at ≈1.1 eV (1127 nm) and weak dip at ≈2.1 eV (590 nm), which correspond to the longitudinal and transverse surface plasmon resonances (SPR), while the phase (Δ) spectrum reveal maximums at these corresponding wavelengths. In this case, tilted AuNRs induce an increment in the photonic light scattering and photonic light trapping correspondingly resulted in the enhancement of the local photon intensity.[26] These phenomena lead to an increase in the excitation of surface plasmons. The SPR wavelengths shift toward longer wavelengths and become broader at isotropic axis. Similar observations were obtained for the real and imaginary parts of the pseudo-dielectric function of AuNR arrays. In those cases, the highly polarizable free charge carriers lead to the sharp increase of the real part of pseudo-dielectric function and the decrease of its imaginary part with increasing photon energy due to electron confinement.[27] It is observed that the pseudo-dielectric function spectrum in **Figure 3**c reveals strong free-electron structure at ≈1.1 eV (1127 nm). The broadening at isotropic axis may also be possibly due to the relaxation time of conduction electrons, which indicates that the directional nanostructured AuNR arrays act like continuous smooth film.[27] Moreover, the polarization of light also contributes to the formation of surface plasmons in AuNR arrays. At anisotropic axis, the p-polarization, which possesses an electric field vector oscillating normal to the plane of AuNRs, mainly excites surface plasmons.[26] However, at isotropic axis, p-polarization cannot excite plasmons enough since it is oriented parallel to AuNRs. In this case, the surface plasmons are mainly excited by s-polarization. Although we have not investigated in detail the tilt angle, length, and density of nanostructures should be taken into account for further understanding of this interesting phenomenon.

Next, the fabricated AuNR arrays were coated with PNIPAAm by initiated-chemical vapor deposition (i-CVD), which is a special class of vapor-phase polymerization technique. Through the utilization of i-CVD, substrates that have 3-D morphologies

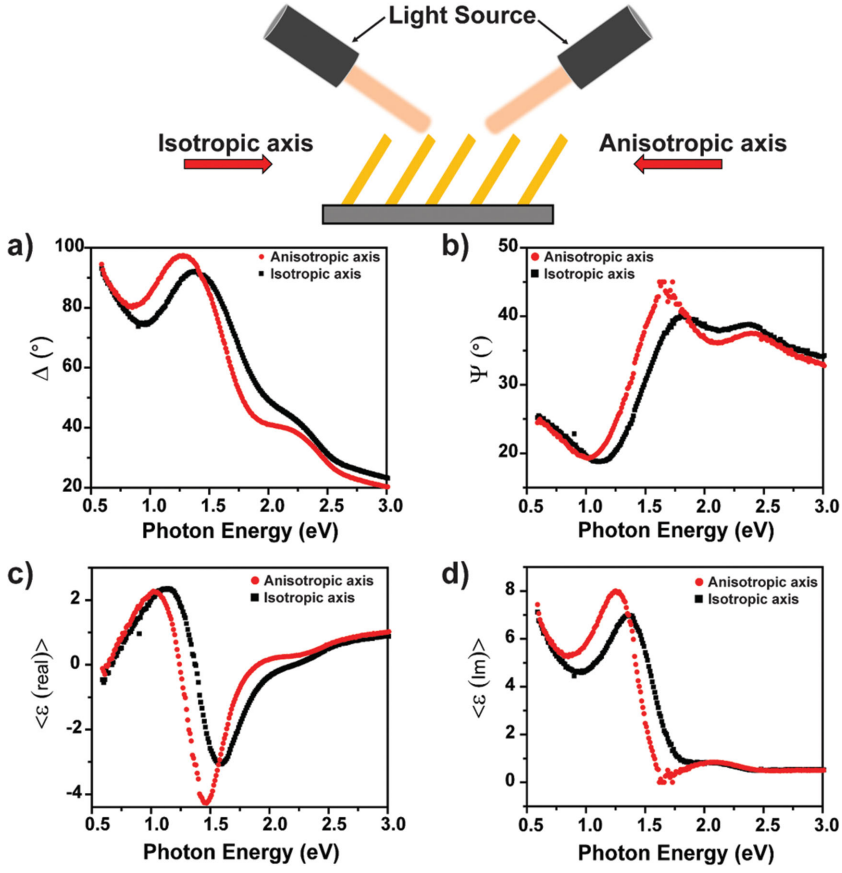

Figure 2. Variations of the ellipsometric parameters a) Δ, b) Ψ, c) real ($\langle\varepsilon_{real}\rangle$), and d) imaginary ($\langle\varepsilon_{Im}\rangle$) parts of the pseudo-dielectric function for the directional AuNR arrays before PNIPAAm coating depending on the direction of incoming light.

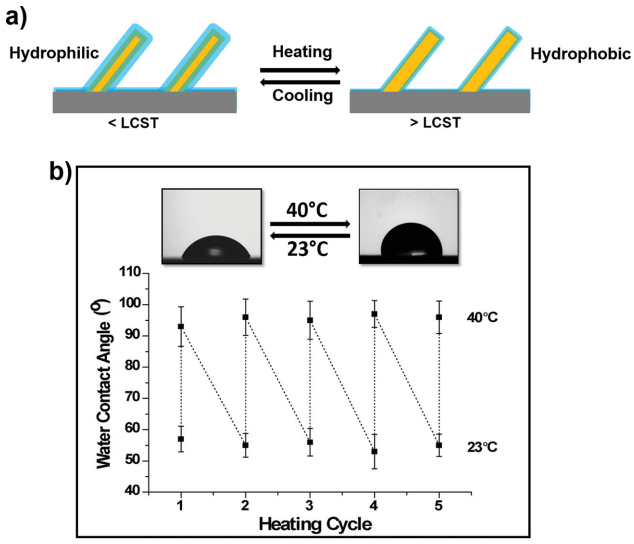

Figure 3. a) Schematic for temperature-dependent wetting transformation of PNIPAAm-coated AuNR array from hydrophilic to hydrophobic and b) water contact angles for five cycles of quick temperature changes between 23 and 40 °C.

(as reported in this work) can be conformally coated, and undesired impurities, degradation of the underlying material, and alteration of mechanical/chemical properties arising from mainly the utilization of solvents can be precisely eliminated.[28, 29] In this respect, PNIPAAm films having a thickness about 58 ± 5 nm were deposited on AuNRs. After polymer deposition, we did not find any change on the morphology of AuNRs, which indicates the conformal coating of PNIPAAm (see Figure S2 in the Supporting Information). The chemical characterization of PNIPAAm layers was carried out with Fourier transform infrared spectrometer (FTIR) and X-ray photoelectron spectrometer (XPS) (see Figure S3a,b in the Supporting Information). FTIR peaks reveal isopropyl C–H stretching at 2973 cm^{-1}, secondary amine N—H stretching at 3320 cm^{-1}, amine C—N—H bending at 1528 cm^{-1}, and C—O stretching at 1664 cm^{-1} indicating complete polymerization. The XPS analysis also shows that the characteristic signal of carbon, oxygen, and nitrogen exist in the spectrum due to PNIPAAm coating on AuNRs. In addition to these, we investigated the optical properties of fabricated AuNR arrays after PNIPAAm coating. It is found that, as expected, the ellipsometric parameters shifted after polymer coating compared with the pristine film due to the changes in the local refractive index (see Figure S4 in the Supporting Information).

The changes in the surface free energy of PNIPAAm on AuNR arrays under conventional heating were investigated through static contact angle measurements (Figure 3a). It is well known that PNIPAAm is a temperature-sensitive polymer which transforms from hydrophilic state to hydrophobic one above its lower critical solution temperature (LCST) of ≈32 °C.[30-33] As expected, the water contact angle value at 23 °C (below LCST) was measured to be ≈55°, while it was approximately 95 at 40 °C (above LCST). At 23 °C, the intermolecular hydrogen bonding between the polymeric structure and water molecules is responsible for the hydrophilic behavior of PNIPAAm. At 40 °C, the temperature increase reduces the intermolecular distance and leads to the prevalence of a strong intramolecular hydrogen bonding between C=O and N—H groups in polymeric structure.[30] Thus, PNIPAAm-coated AuNR arrays show hydrophobicity at high temperatures (above LCST). The repeatability of the temperature-dependent wettability of fabricated surfaces at 23 °C and 40 °C was also tested and a decisive reversibility was observed for five cycles of quick transformations between hydrophilicity and hydrophobicity (Figure 3b).

One of the unique features of plasmonic nanostructures is their ability to generate thermal energy under optical illumination based on strong scattering and absorption of light in the visible and near-infrared region, owing to their localized surface plasmon resonances.[34, 35] Such a conversion provides very rapid and localized heating with high selectivity. Starting from this point, we envisaged that by combining a temperature-sensitive polymeric thin film with a directional AuNR arrays having photothermal properties, we may drive and guide liquid motion at a controlled speed using light illumination (**Figure 4**a). According to our concept, upon a focused light irradiation near the liquid–surface interface, the heat will be generated by the plasmonic AuNR arrays and then transferred from AuNRs to PNIPAAm layer and water droplet. This would result in both a rapid creation of surface free energy heterogeneity due to the transformation of hydrophilic PNIPAAm to hydrophobic one and liquid evaporation from the interface. For conventional heating, which leads to the temperature increase all around the surface, it is expected that the transformation of PNIPAAm from hydrophilic to hydrophobic configuration prevent the liquid motion. However, in our case due to the directional AuNR arrays and focused plasmonic heating, liquid motion will be promoted.

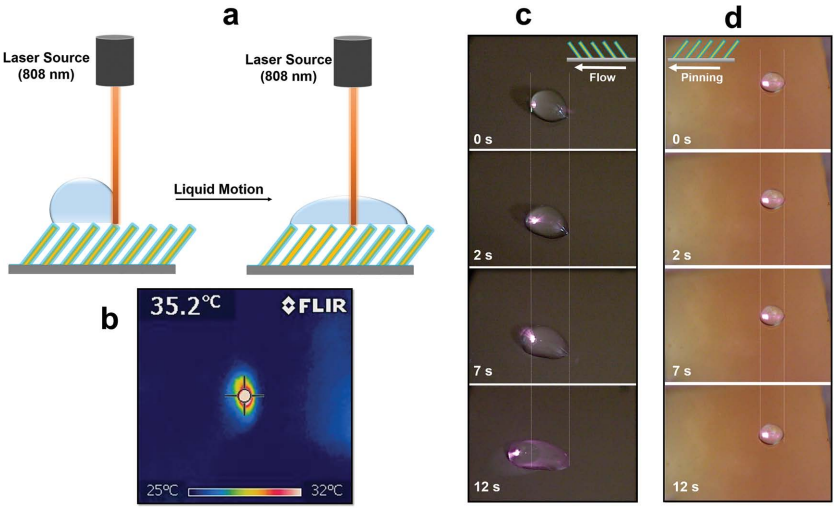

Figure 4. a) Proposed concept illustration for light-driven liquid motion on PNIPAAm-coated AuNR arrays, b) temperature distribution in water with focused laser illumination, c) video prints showing the light-driven water motion at the isotropic, and d) anisotropic orientation of AuNRs.

In this process, the vapor produced by the evaporation of water with focused plasmonic heating first condenses rapidly and tiny water droplets form in contact with the liquid–surface interface.[16] These water droplets then merge with the original liquid body. During this process, thanks to the directional nanostructures, the water on the hydrophobic PNIPAAm tends to move from hydrophobic region to hydrophilic area and assists the advance of the liquid–surface interface. The liquid motion would be continuous if the laser illumination is translated along with the advancing liquid–air interface at a certain direction. When the laser beam is focused on the other side of liquid where the orientation of AuNRs is antiparallel to follow direction, there will be almost no liquid motion because of the pinning. To support our concept, a 20 µL water droplet was placed onto a PNIPAAm-coated AuNRs array and then irradiated with a tunable 808 nm laser beam which was focused on one side of the droplet (the diameter of the focused light beam is ≈200 µm and the average power of the laser is also in the range of 0–2.0 W) (Figure 4a). The wavelength of light (808 nm) that is used to generate thermal energy from plasmonic substrates was chosen due to the fabricated AuNR arrays exhibit a broad surface plasmon absorption band (Figure 2). The temperature distribution on the laser illuminated area was also recorded by using a thermal camera (Figure 4b). The temperature reveals a Gaussian distribution and the highest temperature is about 35 °C at the center of the illuminated circular area (above LCST) whereas the rest of the liquid remains at ≈25 °C (below LCST). In Figure 4c, the laser was focused on the left side of the liquid droplet where the orientation of AuNRs is parallel to the flow direction. Under the laser irradiation, liquid droplet started to flow in the left direction with a speed about 320 µm s^{-1} (see Figure S5 and Movie S1 in the Supporting Information). When the laser irradiation was stopped at any point, no further liquid motion was observed until the irradiation was restarted. After 12 s irradiation, the liquid has elongated by 4.1 mm (Figure 4c). By changing the laser power, we succeeded in controlling the velocity of the liquid motion (see Figure S6 in the Supporting Information). The motion speed may be further increased by adopting microchannels, more accurate light control or different plasmonic nanomaterials with higher photothermal efficiency (see Movie S2 in the Supporting Information). Moreover, as shown in Figure 4d, we did not observe significant liquid motion, when laser beam was focused on the opposite side of liquid where the orientation of AuNRs is antiparallel to follow direction (see Figure S5 in the Supporting Information). The liquid only extended by less than 0.1 mm after 12 s laser illumination. The tilted AuNRs (β = ≈41°) on our fabricated surfaces lead to the unidirectional wetting, thereby providing liquid flow in a single direction. This unique feature of PNIPAAm-coated AuNRs serves to guide the motion of a liquid.

Chaudhury and Whitesides have previously reported that if a surface exhibits a spatial gradient in its surface free energy, a water droplet placed on this surface can be moved uphill against gravity.[36] Inspired by this seminal work, we envisaged that the required gradient in the surface tension for uphill motion of liquid can be generated on our surface through light illumination. When the laser is focused on the upper side of the liquid droplet, where the orientation of AuNRs is parallel to follow direction, hydrophilic PNIPAAm layers on the surface transform to hydrophobic ones, which causes the motion of liquid drop to flow from a hydrophobic region to a hydrophilic region. We observed that upon light illumination, the water droplet moves up the 10° and 24° slopes along the direction of increasing surface free energy with average velocities of ≈113 and ≈78 µm s^{-1}, respectively (**Figure 5**a,b). In order to confirm that the uphill motion of the water is indeed activated by light illumination, we carried out the same experiments in the absence of light illumination and observed that water droplet could not flow uphill at all.

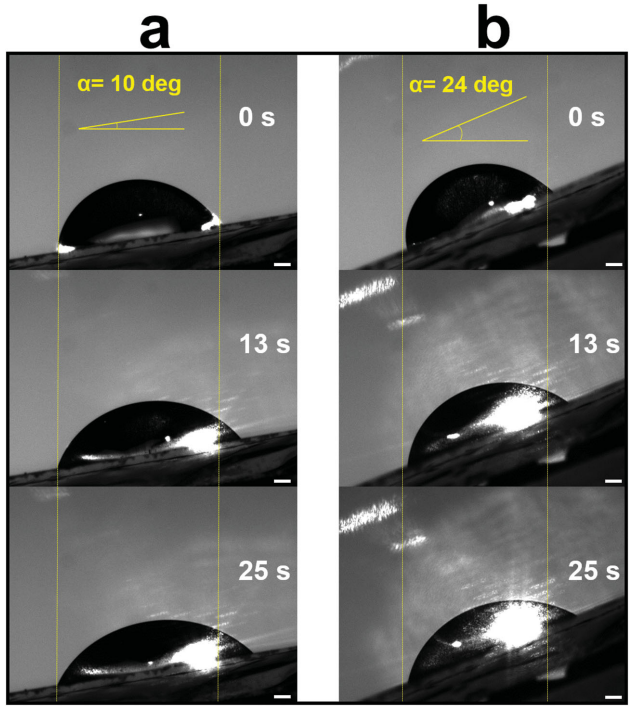

Figure 5. Light-driven uphill motion of a 5 µL water on a) 10° and b) 24° tilted substrates (scale bars = 1 mm).

In summary, we have demonstrated a facile concept for controlling liquid motion through light illumination using temperature-sensitive PNIPAAm-coated plasmonic AuNR arrays. The proposed concept does not only allow the motion and guidance of water through the action of light, but also serves to control the motion speed and direction of the fluid easily. We believe that this work combined with fundamental and applied research will help to understand the direction-dependent wetting properties of materials, light-driven liquid motion, and anisotropic plasmonic behavior. The knowledge will in return guide future design and applications of functional nanomaterials. By manipulating the morphology, wettability, plasmonic properties, and surface chemistry of the fabricated platforms, the light-driven motion capabilities of these platforms can be expanded for various applications.

Experimental Section

Fabrication of 3-D Gold Nanorod Arrays: To fabricate directional gold nanorod (AuNR) arrays, the substrates (i.e., BK7 glass slides or silicon

wafers) are first cut (2.5 × 2.5 cm^2) and washed with deionized water, ethanol, acetone, and piranha solution consecutively. The precleaned substrates are then treated with oxygen plasma at low pressure (0.2 mbar) for 30 min before gold deposition. The directional AuNR arrays are fabricated in a conventional physical vapor deposition system (Nanovak HV, Ankara, Turkey) using a homemade oblique angle deposition equipment. The directional AuNRs are created at the deposition angle of $\alpha = 5°$. The thickness of deposited films is monitored by deposition monitor with 0.5% sensitivity. Base pressure is gained by using a mechanical and turbo pump and monitored via Wide Range Vacuum Gauge Controller. During deposition, the base pressure is fixed at $\approx 8 \times 10^{-6}$ Torr with gold evaporation rate of 0.1 Å s^{-1}. For comparison, smooth gold films having 30 nm Au are also fabricated at $\alpha = 90°$.

Fabricated AuNR arrays are characterized by a QUANTA 400F field emission SEM with an acceleration voltage of 20 kV. The SEM images are then analyzed through the freeware IMAGEJ image analysis software. Plasmonic properties of directional AuNR arrays depending on AuNR orientations (i.e., isotropic and anisotropic axis) are also analyzed by spectroscopic phase modulated ellipsometer (Jobin Yvon-Horiba) with a spectral range from 0.5 to 4.7 eV in steps of 0.01 eV in ambient air at an angle of incidence of 65°. In measurements, the analyzer head focuses the light beam originating from the 75 W Xenon light source on the sample with a polarizing lens. In this configuration, deposited nanofilms are placed one by one on the stage both isotropic and anisotropic axis and $I_s = \sin(2\Psi)\sin(\Delta)$ and $I_c = \sin(2\Psi)\cos(\Delta)$, where Ψ and Δ are conventional ellipsometric angles, are then obtained. It should be noted that ellipsometry does not provide direct information about the dielectric properties of a sample. Therefore, assuming the analyzed sample is a substrate with no overlayers or roughness, pseudo-dielectric functions are extracted from the ellipsometrically measured Ψ and Δ values by applying Equation (1);[37]

$$\langle \varepsilon \rangle = \sin^2\Theta + \sin^2\Theta\tan^2\Theta\,(1 - \tan\Psi e^{i\Delta} / 1 + \tan\Psi e^{i\Delta})^2 \quad (1)$$

where Θ is the angle of incidence.

PNIPAAm Coating with i-CVD: Thin films of PNIPAAm are deposited on the AuNR arrays via i-CVD technique, which is based on free-radical polymerization with precursors in the vapor phase. The monomer and initiator vapors are delivered into a vacuum reactor at a base pressure of 1 mTorr. The heated filaments inside the reactor thermally decompose the initiator molecules, forming *t*-butoxyl radicals. The initiator radicals then react with the vinyl bonds of the monomer molecules adsorbed on the substrate, forming monomer radicals. Continuous delivery of monomer and initiator molecules into the reactor allows the polymer chains to grow at a steady rate. The filaments are maintained at a low temperature to protect the functional groups of the monomer molecules. The low substrate temperatures and lack of solvents in the process enable coating of the delicate substrates conformally. PNIPAAm depositions are performed at the substrate and filament temperatures of 20 °C and 283 °C, respectively. During depositions the reactor pressure is kept at 250 mTorr and the flow rates of NIPAAm, ethylene glycol dimethacrylate, *tert*-butyl peroxide, and N_2 are 1.0, 0.07, 1.02, and 1.1 sccm. The thickness of the coatings is monitored real-time using a laser interferometer. The thickness of the PNIPAAm coatings used in this study is ≈58 nm.

Supporting Information

Supporting Information is available from the Wiley Online Library or from the author.

Acknowledgements

This project was supported by the Scientific and Technological Research Council of Turkey (TUBITAK) Grant Nos. 112T560 and 114Z296. G.D. and G.O.I. acknowledge support from the Turkish Academy of Sciences Distinguished Young Scientist Award (TUBA-GEBIP).

Received: May 5, 2015
Revised: June 5, 2015
Published online: July 14, 2015

[1] G. M. Whitesides, *Nature* **2006**, *442*, 368.
[2] T. M. Squires, S. R. Quake, *Rev. Mod. Phys.* **2005**, *77*, 977.
[3] D. J. Beebe, G. A. Mensing, G. M. Walker, *Annu. Rev. Biomed. Eng.* **2002**, *4*, 261.
[4] D. Psaltis, S. R. Quake, C. Yang, *Nature* **2006**, *442*, 381.
[5] T. Schnedider, J. Kreutz, D. T. Chiu, *Anal. Chem.* **2013**, *85*, 3476.
[6] A. Gunther, K. F. Jensen, *Lab Chip* **2006**, *6*, 1487.
[7] S. Balslev, A. Kristensen, *Opt. Express* **2005**, *13*, 344.
[8] L. Brousse, C. Cohen, T. Nikiforov, A. Chow, A. R. Kopf-Sill, R. Dubrow, J. W. Parce, *Annu. Rev. Biophys. Biomol. Struct.* **2000**, *29*, 155.
[9] J. Atencia, D. J. Beebe, *Nature* **2005**, *437*, 648.
[10] H. A. Stone, A. D. Stroock, A. Ajdari, *Annu. Rev. Fluid Mech.* **2004**, *36*, 381.
[11] L. Y. Yeo, J. R. Friend, *Biomicrofluidics* **2009**, *3*, 012002.
[12] D. Baigl, *Lab Chip* **2012**, *12*, 3637.
[13] G. Lagubeau, M. Le Merrer, C. Clanet, D. Quere, *Nat. Phys.* **2011**, *7*, 395.
[14] K. Ichimura, S. K. Oh, M. Nakagawa, *Science* **2000**, *288*, 1624.
[15] J. Berna, D. A. Leigh, M. Lubomska, S. M. Mendoza, E. M. Perez, P. Rudolf, G. Teobaldi, F. Zerbetto, *Nat. Mater.* **2005**, *4*, 704.
[16] G. L. Liu, J. Kim, Y. Lu, L. P. Lee, *Nat. Mater.* **2006**, *5*, 27.
[17] P. Y. Chiou, H. Moon, H. Toshiyoshi, C. J. Kim, M. C. Wu, *Sens. Actuator, A* **2003**, *104*, 222.
[18] M. Miyauchi, A. Nakajima, T. Watanabe, K. Hashimoto, *Chem. Mater.* **2002**, *14*, 2812.
[19] F. Xia, L. Jiang, *Adv. Mater.* **2008**, *20*, 2842.
[20] S. Wang, Y. Song, L. Jiang, *J. Photochem. Photobiol., C* **2007**, *8*, 18.
[21] S. Kobatake, S. Takami, S. Muto, T. Ishikawa, M. Irie, *Nature* **2007**, *446*, 778.
[22] D. H. Qu, Q. C. Wang, J. Ren, H. A. Tian, *Org. Lett.* **2004**, *6*, 2085.
[23] N. Katsonis, M. Lubomska, M. M. Pollard, B. L. Feringa, P. Rudolf, *Prog. Surf. Sci.* **2007**, *82*, 407.
[24] L. Kubus, H. Erdogan, E. Piskin, G. Demirel, *Soft Matter* **2012**, *8*, 11704.
[25] M. Yilmaz, E. Senlik, E. Biskin, M. S. Yavuz, U. Tamer, G. Demirel, *Phys. Chem. Chem. Phys.* **2014**, *16*, 5563.
[26] L. Kubus, H. Erdogan, S. S. Cetin, E. Biskin, G. Demirel, *ChemCatChem* **2013**, *5*, 2973.
[27] H. T. Beyene, J. W. Weber, M. A. Verheijen, M. C. M. van de Sanden, M. Creatore, *Nano Res.* **2012**, *5*, 513.
[28] G. O. Ince, A. M. Coclite, K. K. Gleason, *Rep. Prog. Phys.* **2012**, *75*, 016501.
[29] G. O. Ince, E. Armagan, H. Erdogan, F. Buyukserin, L. Uzun, G. Demirel, *ACS Appl. Mater. Interfaces* **2013**, *5*, 6447.
[30] S. Kiper, T. Çaykara, G. Demirel, *Eur. Polym. J.* **2006**, *42*, 348.
[31] Y. H. Bae, T. Okano, S. W. Kim, *J. Polym. Sci: Polym. Phys.* **1990**, *28*, 923.
[32] M. Heskins, J. E. Guillent, E. James, *J. Macromol. Sci. Chem.* **1968**, *A2*, 1441.
[33] H. G. Schild, *Prog. Polym. Sci.* **1992**, *17*, 163.
[34] S. Link, M. A. El-Sayed, *Int. Rev. Phys. Chem.* **2000**, *19*, 409.
[35] H. Erdogan, H. Sakalak, M. S. Yavuz, G. Demirel, *Langmuir* **2013**, *29*, 6975.
[36] M. K. Chaudry, G. M. Whitesides, *Science* **1992**, *256*, 1539.
[37] H. Fujiwara, *Spectroscopic Ellipsometry: Principles and Applications*, John Wiley & Sons, Chichester, UK **2007**, p. 189.

